Respiratory Physiology & Neurobiology 265 (2019) 68–75

Contents lists available at ScienceDirect

Respiratory Physiology & Neurobiology

journal homepage: www.elsevier.com/locate/resphysiol

Respiratory fluctuations in pupil diameter are not maintained during cognitive tasks

Nozomu H. Nakamura[a,*], Masaki Fukunaga[b], Yoshitaka Oku[a]

[a] Division of Physiome, Department of Physiology, Hyogo College of Medicine, 1-1, Mukogawa cho, Nishinomiya, Hyogo 663-8501, Japan
[b] Division of Cerebral Integration, Department of System Neuroscience, National Institute of Physiological Sciences, 38 Nishigonaka Myodaiji, Okazaki, Aichi 444-8585, Japan

ARTICLE INFO

Keywords:
Pupillometry
RR interval
Breathing-dependent fluctuation
Parasympathetic
Sympathetic

ABSTRACT

Pupil diameter fluctuation throughout the respiratory cycle is autonomically controlled in the resting state, as pupils dilate during inspiration and constrict during expiration. Furthermore, pupil size is differentially modulated by cognitive states between task engagement and disengagement. To determine whether respiratory-dependent fluctuations in pupil size are maintained during a cognitive task, we employed healthy human subjects performing a delayed matching-to-sample task with a short delay and measured their pupil sizes and R wave-to-R wave intervals (RRIs). We detected respiratory fluctuations in pupil size and the RRI during the delay period immediately before the discrimination stage of the task. During the discrimination stage, the cognitive state with the higher task engagement yielded more pupil dilation. However, respiratory fluctuations in pupil size were abolished, whereas those in the RRI were still discernible during the discrimination stage. Our results suggest that an alternative control mechanism involving the cognitive state associated with task engagement overrides the respiratory-related autonomic control of pupil diameter.

1. Introduction

Respiratory sinus arrhythmia (RSA) is a known natural variation in the R wave-to-R wave interval (RRI) between heartbeats that occurs during a respiratory cycle in animals and humans (Eckberg, 2003; Dergacheva et al., 2010; Larsen et al., 2010) and is used as an accepted index of parasympathetic cardiac vagal tone in the resting state (Gilad et al., 2005; Denver et al., 2007; Tzeng et al., 2009). Meanwhile, pupil diameters fluctuate throughout the respiratory cycle in animals and humans (Borgdorff, 1975; Ohtsuka et al., 1988; reviewed by Häbler et al., 1994): pupil diameter dilates during inspiration and constricts during expiration, actions that are innervated by sympathetic and parasympathetic activities, respectively (Borgdorff, 1975). Like RSA, pupil size respiratory fluctuation is a potential indicator for monitoring autonomic activity.

Pupil diameter is modulated by cognitive processes via the locus coeruleus (LC) and prefrontal cortex (Joshi et al., 2016; Ebitz and Platt, 2015; reviewed by Aston-Jones and Cohen, 2005) and is used as an index of the cognitive or arousal state (Beatty, 1982; Sirois and Brisson, 2014). In particular, changes in pupil size may be linked to two modes of task performance: i) task engagement during high performance, where the detection of known or "matching" events is associated with a decreased baseline pupil diameter, and subsequently, increased pupil dilation, and ii) disengagement from the task (detection of "mismatching" events), which is associated with an increased baseline pupil diameter, and subsequently, less pupil dilation (Richer and Beatty, 1987; Gilzenrat et al., 2010; Otero et al., 2011; de Gee et al., 2014; Papesh et al., 2012).

While visual stimuli and cognitive states are involved in changes in pupil size, whether respiratory fluctuation in pupil size is maintained during cognitive tasks remains unclear (Ohtsuka et al., 1988; reviewed by Häbler et al., 1994). Here, the present study investigated whether respiratory fluctuation in pupil size is discernible during a cognitive task. We employed healthy volunteers to perform a delayed matching-to-sample (DMTS) recognition task (Nakamura et al., 2013; Nakamura and Sauvage, 2016) with a short delay (Olsen et al., 2009; Jeneson et al., 2011) while monitoring changes in their RRIs and pupil diameter a simultaneously with respiration. Specifically, we focused on certain periods of the task, before and during the discrimination stage (the delay and test sections), in which "matching" events may have more pupil dilation than "mismatching" events (Richer and Beatty, 1987; Gilzenrat et al., 2010; Otero et al., 2011; de Gee et al., 2014; Papesh et al., 2012).

* Corresponding author.
E-mail address: no-nakamura@hyo-med.ac.jp (N.H. Nakamura).

https://doi.org/10.1016/j.resp.2018.07.005
Received 22 March 2018; Received in revised form 20 June 2018; Accepted 14 July 2018
Available online 17 July 2018

2. Methods

2.1. Subjects

Fourteen healthy right-handed volunteers (6 males, 8 females; aged 22.7 ± 0.8 years; range 20–30 years) participated in the study. All participants had abstained from caffeine-containing beverages for at least 12 h before the psychophysiological experiment. No subjects were taking medications regularly, and none had known histories of respiratory, cardiovascular, or endocrine diseases. Written informed consent was obtained from all participants. All procedures performed on humans were in accordance with the Declaration of Helsinki (Ethical Principles for Medical Research Involving Human Subjects) and the Ethical Guidelines from Medical and Health Research Involving Human Subjects, Japan, and were approved by the Ethics Committee of Hyogo College of Medicine in Japan (No.1825).

2.2. Apparatus

The inspiratory (I) and expiratory (E) phases of respiratory cycles were continuously recorded via a flow sensor nasal cannula (Flow Nasal Cannula A, Atom Medical, Japan) equipped with a differential pressure transmitter (model KL17, Nagano Keiki, Japan) (Oku and Okada, 2008). An electrocardiogram (ECG) was recorded via lead II (voltage between the left leg and right arm electrodes) using a differential biological amplifier (Bioamp, AD Instruments, Sydney, Australia). Images with pupil diameter changes were acquired with an infrared video camera (1920 × 1080 resolution, 60 Hz frames per second; HC-W870 M, Panasonic, Japan), and subjects were placed at a viewing distance of 75 cm from the computer screen (47.7 cm × 26.8 cm, 1920 × 1080 resolution, 60 Hz refresh rate) under dim light. We measured illuminance with a lux-meter positioned at the same distance from the screen. Illuminance increases were ~1 lx during each figure presentation (baseline was 0 lx; as a reference, changing from the black to white screen in our setup was ~72 lx). The video camera was fixed below the screen, and the distance from the camera lens to the subject's right eye was 62.6 cm (55 cm depth x 30 cm height). The respiratory cycles, ECG, and trigger signals were sampled at 1 kHz using the PowerLab data acquisition system (PowerLab, AD Instruments) and were computed online using LabChart software (LabChart 7.1, AD Instruments).

2.3. Task paradigm

We developed a delayed matching-to-sample (DMTS) version (Nakamura et al., 2013; Nakamura and Sauvage, 2016; Eichenbaum et al., 2007) of a visual recognition task with a short delay for humans (Olsen et al., 2009; Jeneson et al., 2011). The DMTS task consisted of a study section, a delay section, and a test section and followed the DMTS rule. Task paradigms were created using NBS Presentation® software (Presentation 18.3, Neurobehavioral Systems).

The DMTS task required the memorization and recognition of a figure (configuration), its color, its position, and the number of replicated figures shown on a computer screen (47.7 × 26.8 cm, 1920 × 1080 resolution, 60 Hz refresh rate). The shape (configuration) was a circle, triangle, rectangle, cross, crescent, or heart; the color was red, blue, green, yellow, pink, or sky blue; the number of figures was one, two, three, four, five, or six; and the position on the screen was center, right, left, top-center, bottom-right, or bottom-left (Fig. 1A). Thus, 1296 (6 × 6 × 6 × 6 variables) possible combinations existed.

During the study section, each subject was exposed to a series of four of 1296 total figures, which were displayed one at a time on a computer screen under dim light in a darkened room (Fig. 1A and B). After a short delay, each subject was tested three separate times on their ability to distinguish between the figure presented during the study section ("matching figure" or "old figure") and a "mismatching figure" or "new figure" that was one of 1296 figures not presented during the study section (Fig. 1A).

A "matching figure" (or "old figure") was defined as the figure consisting of the same four elements: shape (configuration), color, position, and number of figures presented during the study section. A "mismatching figure" (or "new figure") was defined as a figure that did not contain more than one of the four elements presented during the study section. The subjects pressed the "Z" or "C" key on a standard keyboard using fingers on their left hand once they had identified the figure shown during the test section as a "matching figure" or "mismatching figure", respectively. One "block" of the task was made up of the study section (12 s), delay section (12 s), test section (9 s), and answer section (Fig. 1B). Each subject performed ten blocks of the task (one session), and 15 "matching figures" and 15 "mismatching figures" were presented during the session in random manner. Each subject was informed of the correct answers after the test section.

To increase difficulty of the DMTS task, inter-stimulus intervals (ISIs) between retrieval cues and the exposure durations of the cues were set as follows: i) ISIs were 3 s in duration with three different time lags (0, 300, and 600 ms after a trigger signal, in random order), and ii) the exposure durations of retrieval cues were set from 200 to 500 ms in random order. We then used the test trials with cue exposure durations from 200 to 300 ms (20 total test trials per subject) for further analysis.

2.4. Cognitive and cardiorespiratory parameter data

During the experiments, we measured cognitive parameters – the time of cue exposure, time of button pressing, and accuracy – using NBS Presentation software, and cadiorespiratory parameters – the RRI, onset of every I and E phase, and time of each I and E nasal tidal pressure amplitude peak in the respiratory waveform – using LabChart software. At a preset level, the onset of every I and E phase was defined as the time at which the flow first crossed the basal level and shifted toward the opposite domain by over ± 2 standard deviations from baseline noise after reaching every I and E peak. Thus, the onsets of the I and E phases corresponded to the expiratory-to-inspiratory phase (EI) transition and the inspiratory-to-expiratory phase (IE) transition, respectively. The series of cardiorespiratory parameters in each trial was synchronized with that of cognitive parameters. To identify the distribution of test cues between the I and E phases, the exposure timing of individual test cues was rearranged on a scale according to the I/E circular phase in degrees: 0° represented the EI transition, 180° represented the IE transition, and 360° represented the next EI transition (Fig. 3D), similar to a previous study (Deschênes et al., 2016). We also identified the RRI variations in each respiratory cycle (Tzeng et al., 2009). Generally, the RRI was defined as the interval from an R wave (R_n) to the next R wave (R_{n+1}). Here, an interval from an R wave (R_n) to the previous R wave (R_{n-1}) was defined as RRI (Fig. 1C) because the latter is thought to represent the input to output relationship appropriately. The z-score in each RRI was standardized by mean and standard deviation during the delay or test section in individual subjects and was then used for further analysis.

2.5. Pupil data analysis

Pupil data were synchronized with the time courses of cognitive parameters according to trigger signals at the starting and end points of the task, captured by an infrared video camera. The pupil center position and pupil diameter in an image series were detected using Eye Tracking System software (Gazo, Niigata, Japan). Processing of image series for pupil diameter was performed using Image J software (ImageJ 1.51k, Wayne Rasband, NIH, USA; https://imagej.nih.gov/ij) and Matlab (MathWorks, USA, https://www.mathworks.com) with in-house functions (Wainstein et al., 2017). Data analysis was restricted to the periods of 3000 ms before and after the test trials. Test trials missing more than 50% of the data (due to blinks) were not considered in the

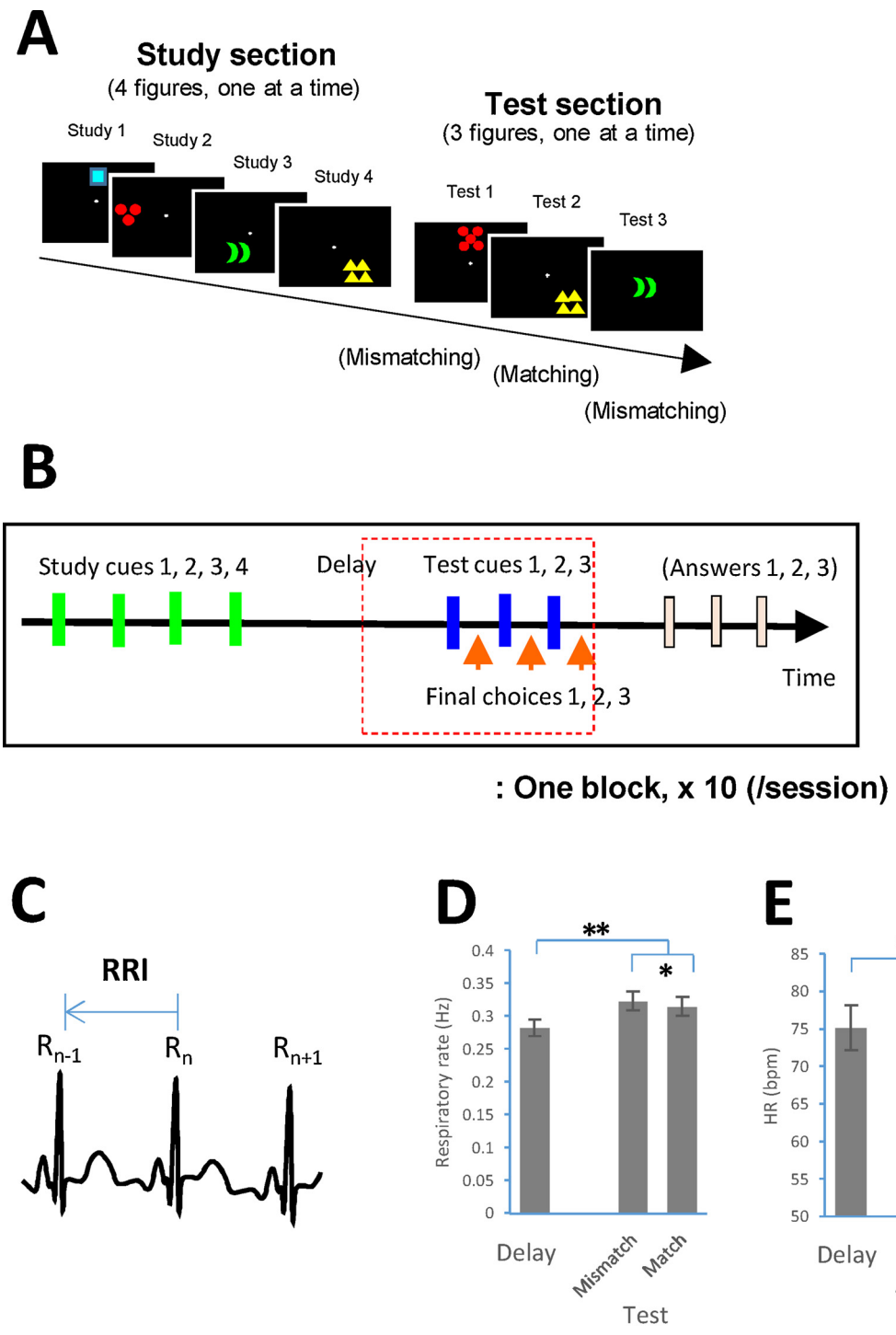

Fig. 1. Visual DMTS task, respiratory rate, and heart rate.
A. Schematic drawings showing examples of figures during the study and test sections of the DMTS task. B. The task is composed of a study section (green bars), a delay section, a test section (blue bars), and an answer section (white bars). Following individual test cues, the subjects press a button (orange arrows) for their decision. Specifically, we focused on the delay and test sections (red dotted rectangle). C. Schematic drawings showing electrocardiograms. The RRI was measured from an R wave (R_n) to the previous R wave (R_{n-1}). D, E. Bar plots showing the respiratory rates (n = 14, D) and heart rates (HR; n = 14, E) during the delay section and the mismatching and matching processes in the test section. * $p < 0.05$, and ** $p < 0.0001$ compared with relevant pairs.

analysis. Trial data were removed when the pupil center position shifted more than 5.5 mm in an image series during the test trial period. Of note, a 5.5-mm shift in the pupil center position in an image induces pupil diameter shrinkage by 0.004%, while the present study showed an approximate 1.5% change in pupil diameter during the test trial. Then, we plotted every 50-ms pupil diameter window in each 3000 ms period before the test section and during the test section. Pupil data surrounding blinks were removed from the time series, and the pupil diameters during these periods were estimated using a linear interpolation. A z-score in each pupil size (every 50-ms window) was standardized by mean and standard deviation during the 3000-ms period of the delay or test section in individual subjects and was then used for further analysis.

2.6. Statistical analysis

Across individual subjects, one-way repeated measures ANOVA and the paired *t*-test were used to assess the significance of differences between relevant pairs. Two-way repeated measures ANOVA was used to evaluate the significance of the main effects and interactions between factors. To confirm whether a dataset of z-scores meets the necessary assumptions for repeated measures ANOVA, we tested normality and sphericity in respiratory fluctuating z-scores by the Shapiro-Wilk normality test and the Mauchly test for sphericity. The nonparametric Friedman test was assessed if normality or sphericity was violated. *Post hoc* comparison was conducted by pairwise comparisons using the paired *t*-test with Bonferroni adjustment or the Wilcoxon signed rank test with Bonferroni adjustment. All statistical analyses were performed using R 3.3.1 software (R Core Team, R Foundation for Statistical Computing, Vienna, Austria, 2016, https://www.R-project.org/).

3. Results

3.1. Delay and test sections during the DMTS task

In the present study, healthy subjects (n = 14) performed the DMTS task, which contained two test trials (see Methods): i) the matching process, in which each subject was tested to discriminate an “old” or “matching” figure presented during the study section; and ii) the mismatching process, in which each subject was tested to discriminate a “new” or “mismatching” figure that was one of 1296 figures not presented during the study section.

We particularly focused on two sections of the task, the delay section and the test section to compare changes in RRI and pupil size before and during the task discrimination stage. One-way repeated measures ANOVA showed that the delay section had a lower respiratory rate and a higher heart rate (HR) than the test section [respiratory: $F(1, 27) = 42.87$, $p < 0.0001$; HR: $F(1, 27) = 29.39$, $p < 0.0001$, Fig. 1D and E]. Moreover, in the test section, the paired *t*-test showed that the matching process had a lower respiratory rate and a higher HR than the mismatching process [respiratory: $t(13) = 2.27$, $p = 0.04$; HR: $t(13) = 2.24$, $p = 0.04$, Fig. 1D and E].

3.2. Respiratory fluctuations in RRI and pupil size during the delay section

We investigated whether respiratory phases in the cycle altered the RRI and pupil size during the delay and test sections (Fig. 1B). We used an “I/E circular phase”, expressed in degrees, based on the convention from a previous study (Deschênes et al., 2016) (Fig. 2A), in which the I phase occurred from 0 to π (IE transition, yellow line), and the E phase occurred from π to 2π (EI transition, red line). The respiratory phases between 0 and π and between π and 2π were based on the time scale.

To identify the RRI oscillation during breathing in the delay section, R waves (R_n) were divided into six phases (0 to 1/3π, 1/3π to 2/3π, 2/3π to π, π to 4/3π, 4/3π to 5/3π, and 5/3 to 2π) in the respiratory cycle (Fig. 2A), and the RRI was then analyzed for respiratory fluctuation (Table 1). To determine whether RRI meets the necessary assumptions for repeated measures ANOVA, we estimated normality and sphericity in respiratory fluctuating RRI z-score by the Shapiro-Wilk normality test and the Mauchly test for sphericity: RRI z-scores had normality and sphericity during the delay sections. Thus, we used repeated measures ANOVA for further analysis. One-way repeated measures ANOVA showed that the RRI z-scores fluctuated during the respiratory cycle [$F(5, 65) = 44.54$, $p < 0.00001$]. *Post hoc* comparison by pairwise comparisons using the paired *t*-test with Bonferroni adjustment showed that RRIs in the 5/3π–2π and 0–1/2π phases were higher than RRIs in the 2/3π–4/3π phases ($ps < 0.0002$, Fig. 2B).

Pupil sizes were divided into six phases in the respiratory cycle during the delay section (Table 2). Then, pupil size z-scores were compared in each 200-ms window. The Shapiro-Wilk test showed that pupil diameter had normality during the test sections, but the Mauchly test did not show sphericity in pupil diameter during the test section ($W = 0.034$, $p = 0.02$). The nonparametric Friedman test showed that pupil diameter fluctuated during the respiratory cycle [$\chi^2(5) = 13.03$, $p = 0.02$; of note, one-way repeated measures ANOVA showed a similar effect, $F(5, 50) = 2.98$, $p = 0.02$], although *post hoc* comparison by the nonparametric Wilcoxon signed rank test with Bonferroni adjustment did not show differences in the phase points (Fig. 2C). These results revealed that both the RRI and pupil size oscillated simultaneously with the respiratory cycle immediately before the test section of the task.

3.3. Respiratory fluctuations in RRI and pupil size during the test section

Pupil diameter is known to be differentially affected by the matching and mismatching task processes, with the matching process having more pupil dilation than the mismatching process (Richer and Beatty, 1987; Gilzenrat et al., 2010; Otero et al., 2011; de Gee et al., 2014; Papesh et al., 2012). Here, we investigated whether the test section alters the respiratory fluctuation in pupil size.

The paired *t*-test revealed no differences in the exposure times of visual cues and RT between the mismatching and matching processes [exposure: $t(13) = 0.55$, n.s.; RT: $t(13) = 1.32$, n.s., Fig. 3A and B]. Meanwhile, the mismatching process exhibited higher accuracy than the matching process [$t(13) = 4.38$, $p = 0.0007$, paired *t*-test, Fig. 3C]. We plotted the starting points (i.e., the time when the test cue was first presented) of individual test cues with the RT against the I/E circular phase (Fig. 3D), which indicated that the test cue onset scattered the distribution during the respiratory cycle.

RRI was divided into six phases in the respiratory cycle (Table 1). The Shapiro-Wilk test mostly showed normality in the RRI during the test sections, except in mismatching in one phase (1/3π to 2/3π: $W = 0.81$, $p = 0.006$). The Mauchly test showed sphericity in the RRI during the test section. Thus, repeated measures ANOVA was conducted for further analysis. Two-way repeated measures ANOVA of the main effects of process and phase showed that the mismatching process had a higher RRI z-score than the matching process, and the RRIs in both processes fluctuated similarly in the respiratory cycle [process: $F(1, 139) = 10.2$, $p = 0.002$; phase: $F(5, 139) = 29.4$, $p < 0.00001$; phase x process interaction: $F(5, 139) = 0.77$, n.s., Fig. 3E]. *Post hoc* comparison by pairwise comparisons using the paired *t*-test with Bonferroni adjustment showed that RRIs in the 5/3π–2π and 0–1/2π phases were higher than RRIs in the 2/3π–4/3π phases in the matching and mismatching processes ($ps < 0.00001$), which had similar tendencies to those during the delay section (see Fig. 2B). These findings revealed that the matching process had a higher HR (1/RRI) than the mismatching process during the test section.

Regarding changes in pupil size between the matching and mismatching processes, there was normality, except in the mismatching process in the 1600-ms window ($W = 0.86$, $p = 0.03$, Shapiro-Wilk normality test) and except in the matching process in 400-ms ($W = 0.87$, $p = 0.04$) and 2600-ms ($W = 0.87$, $p < 0.05$) windows. Two-way repeated measures ANOVA showed the main effects of process [$F(1, 403) = 27.68$, $p < 0.00001$] and time with a 200-ms window [$F(15, 403) = 290.9$, $p < 0.00001$], but no significant interaction between the process and time was observed [$F(15, 403) = 1.02$, n.s., Fig. 3F]. The paired *t*-test with Bonferroni adjustment showed that the matching process had a higher pupil size z-score than the mismatching process at 0.6 s [$t(13) = 3.62$, $p < 0.05$; mean ± S.E.M (mm diameter): matching: 6.240 ± 0.403, mismatching: 6.150 ± 0.406].

To further determine whether pupil diameter fluctuates simultaneously with respiration during the test section, we extracted changes in pupil size during two specific periods: i) Period A, which had a peak pupil constriction from 0.6 to 0.95 s (0.4 s duration) following the onset of visual cues; and ii) Period B, the recovery period from 2.1 to 2.45 s (0.4 s duration, Fig. 3F). During Periods A and B of the test section,

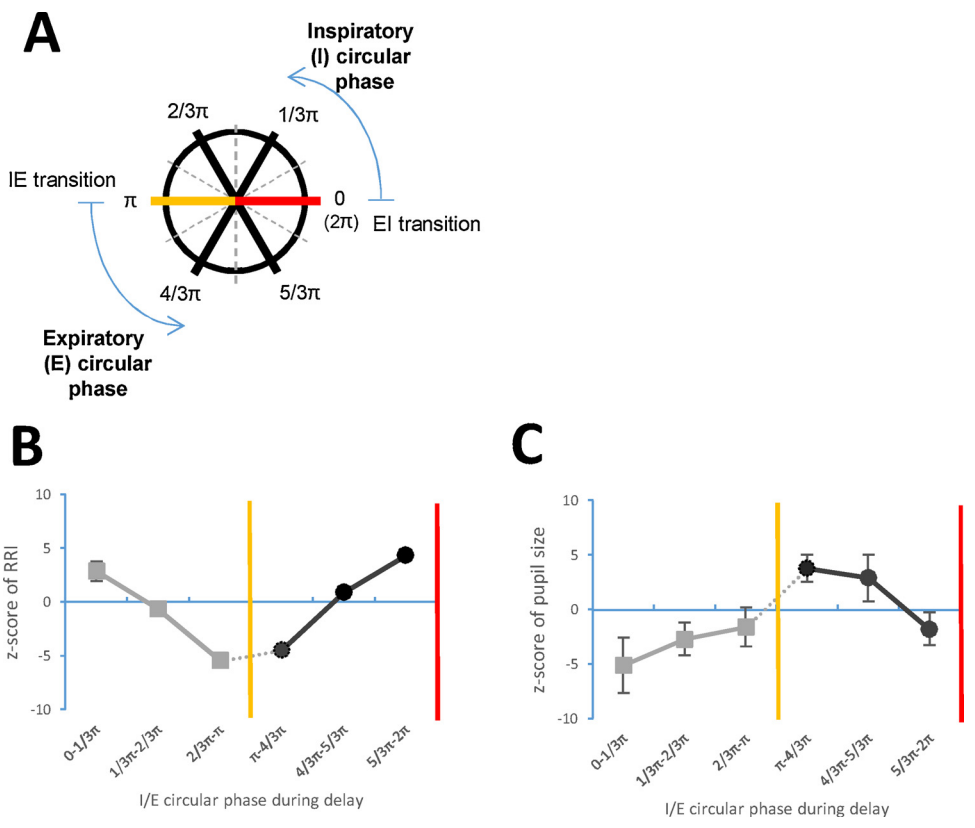

Fig. 2. Respiratory fluctuations in the RRI and pupil size during the delay section.
A. The I/E circular phase is indicated in degrees, where the I phase starts at the EI transition (0, red line) and ends at the IE transition (π, red line), and the E phase starts at the IE transition and ends at the EI transition (2π). B. A line plot showing RRI z-score throughout the I/E circular phase during the respiratory cycle (n = 14). C. Line plots showing pupil size z-scores throughout the I/E circular phase during the respiratory cycle (n = 11).

pupil sizes were divided into six phases in the respiratory cycle (Table 2). Pupil diameter z-score had normality during the test sections, except in mismatching or matching in one phase during Period A (mismatching in π to 4/3π: $W = 0.74$, $p = 0.001$; matching in 4/3π to 5/3π: $W = 0.83$, $p = 0.01$, Shapiro-Wilk test), and except in mismatching or matching in one phase during Period B (mismatching in π to 4/3π: $W = 0.87$, $p < 0.05$; matching in π to 4/3π: $W = 0.84$, $p = 0.01$). The Mauchly test revealed sphericity in pupil diameter during both Periods A and B.

During Period A, two-way repeated measures ANOVA showed the main effect of process with pupil size z-score [$F(1, 133) = 5.65$, $p = 0.02$] but no main effect of phase [$F(5, 133) = 1.10$, n.s.] and no significant interactions between the process and phase were observed [$F(5, 133) = 2.18$, n.s., Fig. 3G]. The paired *t*-test with Bonferroni adjustment showed that the matching process had a higher pupil size z-score than the mismatching process in 1/3π–2/3π [$t(10) = 4.24$, $p = 0.01$]. One-way repeated measures ANOVA showed no respiratory oscillation in the mismatching process [$F(5, 57) = 0.74$, n.s.], whereas the matching process oscillated during the respiratory cycle [$F(5, 63) = 2.36$, $p < 0.05$, Fig. 3G]. However, within the matching process, *post hoc* comparison by pairwise comparisons using the paired *t*-test with Bonferroni adjustment did not clearly show the differences in the phases.

During Period B, pupil sizes were divided into six phases in the respiratory cycle (Table 2). No differences were observed between the matching and mismatching processes during the respiratory phase [process: $F(1, 135) = 0.15$, n.s.; phase: $F(5, 135) = 0.33$, n.s.; process x phase interaction: $F(5, 135) = 1.14$, n.s., Fig. 3H]. These results revealed that during the test section, the matching process maintained more pupil dilation than the mismatching process following visual cue exposure. Moreover, the pupil diameter fluctuated in opposite directions for a very short period (Period A) immediately after cue exposure during the matching process in the task, whereas the pupil diameter during the mismatching process did not fluctuate.

4. Discussion

The present study showed that during the discrimination stage of the DMTS task, the cognitive state abolished respiration-dependent pupil diameter fluctuation, whereas the respiration-dependent RRI fluctuation was maintained. However, the cognitive state with the higher task engagement (matching process) yielded more pupil dilation than that with the lower task engagement (mismatching process), presumably mediated by the LC and prefrontal cortex pathways (Joshi et al., 2016; Ebitz and Platt, 2015; reviewed by Aston-Jones and Cohen, 2005). These results suggest that a regulatory mechanism involving the LC and prefrontal cortex might override the respiratory-related autonomic control of pupil diameter during cognitive tasks.

4.1. Modulations in pupil diameter during the task

We have demonstrated how pupil diameter is modulated during a cognitive task. In the present study, healthy subjects performed the DMTS task under dim light, in which exposure to visual cues was enhanced. Although visual stimuli, which were independent of respiration and the cognitive state, may have aligned or reset changes in pupil size at the beginning of the discrimination stage, the cognitive state yielded different pupil modulations between the matching and mismatching processes. Meanwhile, respiration-dependent pupil fluctuation disappeared during the discrimination stage. Our results indicated that the mechanism controlling pupil size in the cognitive or arousal state worked during the task regardless of visual stimulus disturbances under dim light.

Previous studies have shown that pupil diameter is differentially modulated by task performance, which may reflect activities in the LC and prefrontal cortex (Joshi et al., 2016; Ebitz and Platt, 2015). These modulations are suggested to be linked by two modes, phasic and tonic LC activities (Usher et al., 1999; Gilzenrat et al., 2010; reviewed by Aston-Jones and Cohen, 2005): i) phasic LC activity is typically associated with decreases in baseline pupil diameter in response to task

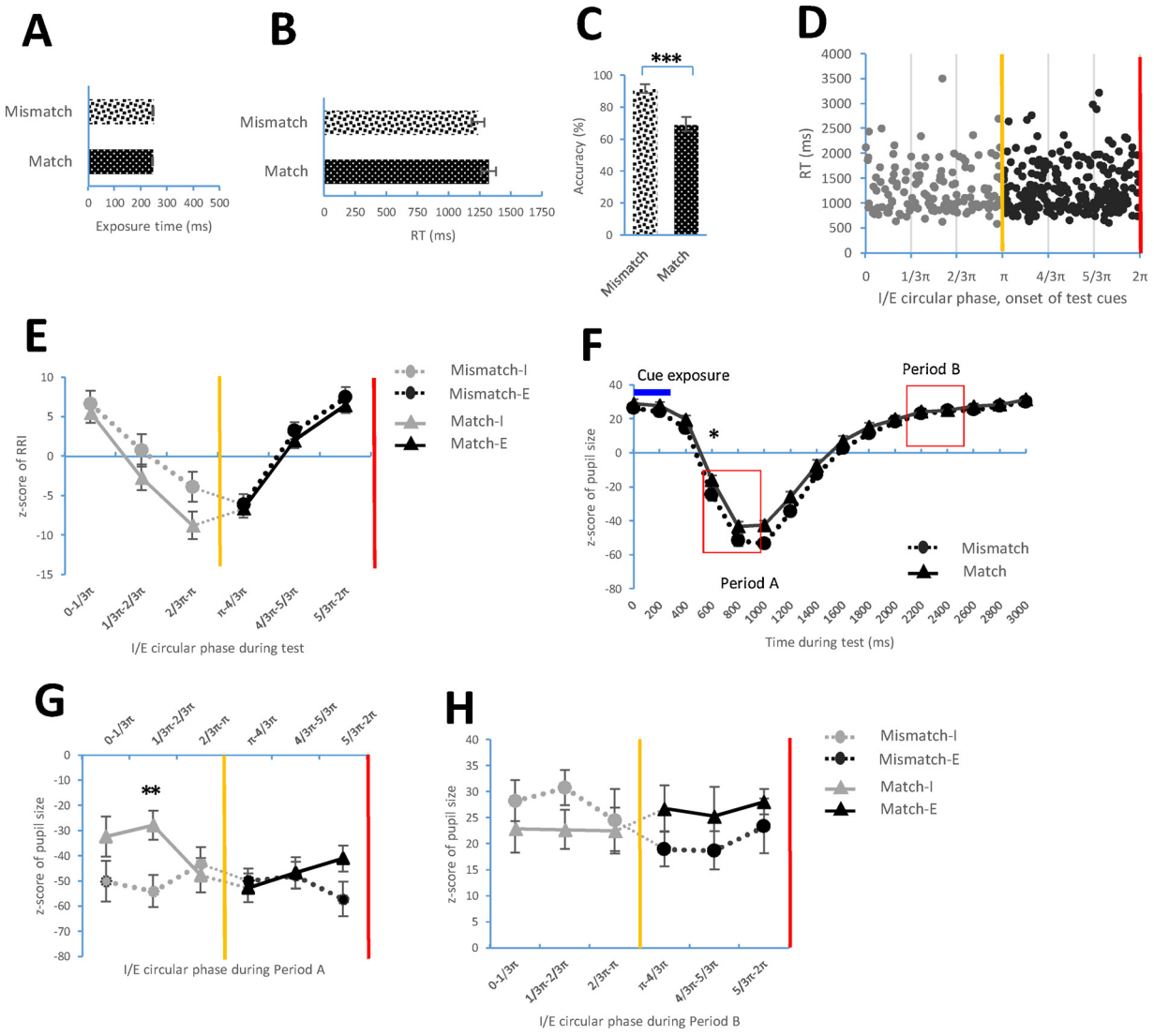

Fig. 3. Respiratory fluctuations in the RRI and pupil size during the test section.
A-E. Bar plots comparing the test cue exposure time (n = 14, A), RT (n = 14, B), and accuracy (n = 14, C) between the mismatching and matching processes during the test section. D. Scatter plots indicating the onsets of individual test cues with RT against the I/E circular phase. E. Line plots showing RRI z-scores between the mismatching and matching processes throughout the I/E circular phase during the respiratory cycle (n = 14). F. Line plots showing pupil size z-scores between the mismatching and matching processes immediately after onset of the test cue exposure (blue line) during the test section (n = 14). G, H. Line plots showing pupil size z-scores between the mismatching and matching processes in Period A (G) and Period B (H) during the test section throughout the I/E circular phase during the respiratory cycle (n = 14). * $p < 0.05$ compared with relevant pairs.

engagement during high performance, and ii) tonic LC activity is associated with increased baseline pupil diameter, the absence of phasic responses, and task degradation in response to disengagement from the task.

Meanwhile, the respiratory fluctuation in pupil size may originate during the activation of the preBötzinger complex (preBötC), a primary respiratory rhythm generator localized in the ventrolateral medulla, the neurons of which generate phasic activities at the onset of I (EI transition, Feldman et al., 2013; Smith et al., 2013). The EI transition-synchronized activation in the heart may play an important role in

Table 1
Respiratory fluctuations in RRI during the delay and test sections.

Respiratory phase	I phase			E phase		
	0–1/3π	1/3π–2/3π	2/3π–π	π–4/3π	4/3π–5/3π	5/3π–2π
mean ± S.E.M (ms)						
Delay	846.5 ± 40.5	824.4 ± 36.6	787.2 ± 33.0	797.9 ± 33.6	835.4 ± 35.8	860.7 ± 37.6
Test						
Mismatching	859.3 ± 37.8	835.5 ± 34.4	799.8 ± 31.7	807.9 ± 29.4	847.9 ± 38.6	863.5 ± 35.7
Matching	859.2 ± 45.4	831.3 ± 31.6	799.1 ± 37.6	801.6 ± 31.9	839.0 ± 39.4	857.6 ± 39.4

Table 2
Respiratory fluctuations in pupil diameter during the delay and test sections.

Respiratory phase	I phase			E phase		
	0–1/3π	1/3π–2/3π	2/3π–π	π–4/3π	4/3π–5/3π	5/3π–2π
mean ± S.E.M (mm)						
Delay	6.895 ± 0.523	6.921 ± 0.513	6.934 ± 0.516	6.982 ± 0.515	6.961 ± 0.527	6.905 ± 0.527
Test (0.60 to 0.95 s)						
Mismatching	5.979 ± 0.428	6.131 ± 0.450	6.088 ± 0.467	5.961 ± 0.454	6.031 ± 0.405	5.803 ± 0.427
Matching	6.205 ± 0.492	6.259 ± 0.435	6.031 ± 0.401	5.976 ± 0.386	6.035 ± 0.414	6.104 ± 0.430
Test (2.10 to 2.45 s)						
Mismatching	6.946 ± 0.409	7.057 ± 0.450	6.652 ± 0.490	6.818 ± 0.421	6.862 ± 0.414	6.875 ± 0.439
Matching	6.874 ± 0.410	6.874 ± 0.412	6.819 ± 0.496	6.931 ± 0.414	6.897 ± 0.421	6.929 ± 0.404

cardiorespiratory coupling (Galletly and Larsen, 1997; Tzeng et al., 2003; Frideman et al., 2012). Moreover, the I phase-dependent activation of neurons in the olfactory bulb, somatosensory cortex, and hippocampus might be involved in sniffing, whisking, and odor discrimination (Cury and Uchida, 2010; Shusterman et al., 2011; Deschênes et al., 2016; Nguye Chi et al., 2016). A recent study demonstrated that the preBötC has efferent projections to the LC, and ablation of these projections leaves breathing intact; however, it decreases the time spent in the attentional and active states (Yackle et al., 2017). These studies suggest a potential pathway for pupil regulation mediated by the LC and prefrontal cortex from the preBötC; however, further work is needed to elucidate the physiological mechanisms underlying respiratory fluctuation in pupil size during cognitive tasks.

4.2. Potential mechanisms underlying respiratory fluctuations

Changes in pupil diameter are caused by two smooth muscles in the iris: the sphincter (or constrictor) and dilator pupillae. The dilator muscle is under the adrenergic control of the sympathetic nervous system from the superior sympathetic ganglion, while the constrictor pupillae is innervated by cholinergic fibers of the parasympathetic system from the parasympathetic oculomotor complex or the Edinger-Westphal nucleus (Laeng et al., 2012; Sirois and Brisson, 2014). However, the detailed mechanisms underlying respiratory-synchronized pupil diameters remain unknown.

Previous studies have identified the physiological mechanism of RSA or RRI fluctuations. The firing pattern of parasympathetic cardiac vagal neurons in the nucleus ambiguus is known to be tonically active, with a firing pattern that is synchronous with the cardiac pulse (Dergacheva et al., 2010). The synchronous pattern of the parasympathetic cardiac vagal tone is innervated by glutamatergic and GABAergic synaptic inputs from the nucleus tractus solitarius (NTS). Cardiac vagal neurons are inhibited by spontaneous increases in GABAergic (and glycinergic) synaptic inputs during inspiration (Wang et al., 2001; Neff et al., 2003). The increases in GABAergic synaptic inputs, mediated by beta 2 nicotinic acetylcholine receptor activation (Neff et al., 2003), are presumably located in the presynaptic termini of GABAergic neurons (Wang et al., 2003). Although the stimulation of afferents in the vagus nerve evokes both glutamatergic and GABAergic responses in cardiac vagal neurons (Evans et al., 2003), the GABAergic pathway evoked by the vagus nerve or NTS stimulation is likely involved in respiratory-dependent RRI fluctuations (Dergacheva et al., 2010). Moreover, an antagonist of muscarinic acetylcholine receptors, atropine is known to decrease respiratory RRI fluctuation in healthy subjects in the resting state (Warner et al., 1986; Hrushesky, 1991; Denver et al., 2007). Consequently, parasympathetic activity from the vagus nerve or NTS is thought to be the dominant source of RSA or RRI variability. However, the reliability of RSA or RRI fluctuations during the performance of cognitive and mental stress tasks is still being deliberated (Lackner et al., 2011; Niizeki and Saitoh, 2012). Further elucidating the biological interactions between the nucleus ambiguus and NTS is important for determining respiratory modulations of the RRI, together with respiratory modulations of pupil diameter in the Edinger-Westphal nucleus and its related brain areas.

5. Conclusion

Our results indicated that in healthy humans, respiratory fluctuation in the RRI was maintained, whereas pupil diameter did not show evidence of respiratory fluctuation during the DMTS task. The cognitive state with the higher task engagement had more pupil dilation, suggesting that the cognitive state might modulate respiratory fluctuations in pupil diameter via a different regulatory mechanism. These findings may provide the basis for understanding the mechanisms of pupil size during cognitive task performances.

Author contribution

NHN contributed to the study design; NHN contributed to acquisition of data; NHN, MF, and YO contributed to methodology and data analysis; NHN contributed to drafting of manuscript; NHN, MF and YO discussed the results and contributed to the final manuscript.

Competing financial interest

All authors declare no competing financial interests.

Acknowledgements

This work was supported by grants from a Grant-in-Aid for Scientific Research 15K12055 in the Japan Society for the Promotion of Science (YO), a Grant-in-Aid for Researchers 2015 in the Hyogo College of Medicine (NHN), the Cooperative Study Program of National Institute for Physiological Sciences (NHN), and the Takeda Science Foundation, 2016 (NHN). We thank Genevieve Yuen (Weill Cornell Medicinal College, New York, NY, USA) for comments on the manuscript.

References

Aston-Jones, G., Cohen, J.D., 2005. An integrative theory of locus coeruleus-norepinephrine function: adaptive gain and optimal performance. Annu. Rev. Neurosci. 28, 403–450.
Beatty, J., 1982. Task-evoked pupillary responses, processing load, and the structure of processing resources. Psychol. Bull. 91, 276–292.
Borgdorff, P., 1975. Respiratory fluctuations in pupil size. Am. J. Physiol. 228, 1094–1102.
Cury, K.M., Uchida, N., 2010. Robust odor coding via inhalation-coupled transient activity in the mammalian olfactory bulb. Neuron 68, 570–585.
de Gee, J.W., Knapen, T., Donner, T.H., 2014. Decision-related pupil dilation reflects upcoming choice and individual bias. Proc. Natl. Acad. Sci. U. S. A. 111, E618–E625.
Denver, J.W., Reed, S.F., Porges, S.W., 2007. Methodological issues in the quantification

of respiratory sinus arrhythmia. Biol. Psychol. 74, 286–294.
Dergacheva, O., Griffioen, K.J., Neff, R.A., Mendelowitz, D., 2010. Respiratory modulation of premotor cardiac vagal neurons in the brainstem. Respir. Physiol. Neurobiol. 174, 102–110.
Deschênes, M., Takatoh, J., Kurnikova, A., Moore, J.D., Demers, M., Elbaz, M., Furuta, T., Wang, F., Kleinfeld, D., 2016. Inhibition, not excitation, drives rhythmic whisking. Neuron 90, 374–387.
Ebitz, R.B., Platt, M.L., 2015. Neuronal activity in primate dorsal anterior cingulate cortex signals task conflict and predicts adjustments in pupil-linked arousal. Neuron 85, 628–640.
Eckberg, D.L., 2003. The human respiratory gate. J. Physiol. 548, 339–352.
Eichenbaum, H., Yonelinas, A.P., Ranganath, C., 2007. The medial temporal lobe and recognition memory. Annu. Rev. Neurosci. 30, 123–152.
Evans, C., Baxi, S., Neff, R., Venkatesan, P., Mendelowitz, D., 2003. Synaptic activation of cardiac vagal neurons by capsaicin sensitive and insensitive sensory neurons. Brain Res. 979, 210–215.
Feldman, J.L., Del Negro, C.A., Gray, P.A., 2013. Understanding the rhythm of breathing: so near, yet so far. Annu. Rev. Physiol. 75, 423–452.
Frideman, L., Dick, T.E., Jacono, F.J., Loparo, K.A., Yeganeh, A., Fishman, M., Wilson, C.G., Strohl, K.P., 2012. Cardio-ventilatory coupling in young healthy resting subjects. J. Appl. Physiol. 112, 1248–1257.
Galletly, D.C., Larsen, P.D., 1997. Cardioventilatory coupling during anaesthesia. Br. J. Anaesth. 79, 35–40.
Gilad, O., Swenne, C.A., Davrath, L.R., Akselrod, S., 2005. Phase-averaged characterization of respiratory sinus arrhythmia pattern. Am. J. Physiol. Heart Circ. Physiol. 288, H504–H510.
Gilzenrat, M.S., Nieuwenhuis, S., Jepma, M., Cohen, J.D., 2010. Pupil diameter tracks changes in control state predicted by the adaptive gain theory of locus coeruleus function. Cogn. Affect Behav. Neurosci. 10, 252–269.
Häbler, H.J., Jänig, W., Michaelis, M., 1994. Respiratory modulation in the activity of sympathetic neurons. Prog. Neurobiol. 43, 567–606.
Hrushesky, W.J., 1991. Quantitative respiratory sinus arrhythmia analysis. A simple noninvasive, reimbursable measure of cardiac wellness and dysfunction. Ann. N. Y. Acad. Sci. 618, 67–101.
Jeneson, A., Mauldin, K.N., Hopkins, R.O., Squire, L.R., 2011. The role of the hippocampus in retaining relational information across short delays: the importance of memory load. Learn. Mem. 18, 301–305.
Joshi, S., Li, Y., Kalwani, R.M., Gold, J.I., 2016. Relationships between pupil diameter and neuronal activity in the locus coeruleus, colliculi, and cingulate cortex. Neuron 89, 221–234.
Lackner, H.K., Papousek, I., Batzel, J.J., Roessler, A., Scharfetter, H., Hinghofer-Szalkay, H., 2011. Phase synchronization of hemodynamic variables and respiration during mental challenge. Int. J. Psychophysiol. 79, 401–409.
Laeng, B., Sirois, S., Gredebäck, G., 2012. Pupillometry: a window to the preconscious? Perspect. Psychol. Sci. 7, 18–27.
Larsen, P.D., Tzeng, Y.C., Sin, P.Y., Galletly, D.C., 2010. Respiratory sinus arrhythmia in conscious humans during spontaneous respiration. Respir. Physiol. Neurobiol. 174, 111–118.
Nakamura, N.H., Sauvage, M.M., 2016. Encoding and reactivation patterns predictive of successful memory performance are topographically organized along the longitudinal axis of the hippocampus. Hippocampus 26, 67–75.
Nakamura, N.H., Flasbeck, V., Maingret, N., Kitsukawa, T., Sauvage, M.M., 2013. Proximodistal segregation of nonspatial information in CA3: preferential recruitment of a proximal CA3-distal CA1 network in nonspatial recognition memory. J. Neurosci. 33, 11506–11514.
Neff, R.A., Wang, J., Baxi, S., Evans, C., Mendelowitz, D., 2003. Respiratory sinus arrhythmia: endogenous activation of nicotinic receptors mediates respiratory modulation of brainstem cardioinhibitory parasympathetic neurons. Circ. Res. 93, 565–572.
Nguyen Chi, V., Müller, C., Wolfenstetter, T., Yanovsky, Y., Draguhn, A., Tort, A.B., Brankačk, J., 2016. Hippocampal respiration-driven rhythm distinct from theta oscillations in awake mice. J. Neurosci. 36, 162–177.
Niizeki, K., Saitoh, T., 2012. Incoherent oscillations of respiratory sinus arrhythmia during acute mental stress in humans. Am. J. Physiol. Heart Circ. Physiol. 302, H359–H367.
Ohtsuka, K., Asakura, K., Kawasaki, H., Sawa, M., 1988. Respiratory fluctuations of the human pupil. Exp. Brain Res. 71, 215–217.
Oku, Y., Okada, M., 2008. Periodic breathing and dysphagia associated with a very localized lateral medullary infarction. Respirology 13, 608–610.
Olsen, R.K., Nichols, E.A., Chen, J., Hunt, J.F., Glover, G.H., Gabrieli, J.D., Wagner, A.D., 2009. Performance-related sustained and anticipatory activity in human medial temporal lobe during delayed match-to-sample. J. Neurosci. 29, 11880–11890.
Otero, S.C., Weekes, B.S., Hutton, S.B., 2011. Pupil size changes during recognition memory. Psychophysiology 48, 1346–1353.
Papesh, M.H., Goldinger, S.D., Hout, M.C., 2012. Memory strength and specificity revealed by pupillometry. Int. J. Psychophysiol. 83, 56–64.
Richer, F., Beatty, J., 1987. Contrasting effects of response uncertainty on the task-evoked pupillary response and reaction time. Psychophysiology 24, 258–262.
Shusterman, R., Smear, M.C., Koulakov, A.A., Rinberg, D., 2011. Precise olfactory responses tile the sniff cycle. Nat. Neurosci. 14, 1039–1044.
Sirois, S., Brisson, J., 2014. Pupillometry. Wiley. Interdiscip. Rev. Cogn. Sci. 5, 679–692.
Smith, J.C., Abdala, A.P., Borgmann, A., Rybak, I.A., Paton, J.F., 2013. Brainstem respiratory networks: building blocks and microcircuits. Trends Neurosci. 36, 152–162.
The R Core Team, 2016. R: A Language and environmental for statistical computing. Reference index, Version 3. 3 .1 1–3507.
Tzeng, Y.C., Larsen, P.D., Galletly, D.C., 2003. Cardioventilatory coupling in resting human subjects. Exp. Physiol. 88, 775–782.
Tzeng, Y.C., Sin, P.Y., Galletly, D.C., 2009. Human sinus arrhythmia: inconsistencies of a teleological hypothesis. Am. J. Physiol. Heart Circ. Physiol. 296, H65–H70.
Usher, M., Cohen, J.D., Servan-Schreiber, D., Rajkowski, J., Aston-Jones, G., 1999. The role of locus coeruleus in the regulation of cognitive performance. Science 283, 549–554.
Wainstein, G., Rojas-Líbano, D., Crossley, N.A., Carrasco, X., Aboitiz, F., Ossandón, T., 2017. Pupil size tracks attentional performance in attention-deficit/hyperactivity disorder. Sci. Rep. 7, 8228.
Wang, J., Irnaten, M., Mendelowitz, D., 2001. Characteristics of spontaneous and evoked GABAergic synaptic currents in cardiac vagal neurons in rats. Brain Res. 889, 78–83.
Wang, J., Wang, X., Irnaten, M., Venkatesan, P., Evans, C., Baxi, S., Mendelowitz, D., 2003. Endogenous acetylcholine and nicotine activation enhances GABAergic and glycinergic inputs to cardiac vagal neurons. J. Neurophysiol. 89, 2473–2481.
Warner, M.R., deTarnowsky, J.M., Whitson, C.C., Loeb, J.M., 1986. Beat-by-beat modulation of AV conduction. II. Autonomic neural mechanisms. Am. J. Physiol. 251, H1134–H1142.
Yackle, K., Schwarz, L.A., Kam, K., Sorokin, J.M., Huguenard, J.R., Feldman, J.L., Luo, L., Krasnow, M.A., 2017. Breathing control center neurons that promote arousal in mice. Science 355, 1411–1415.